Dr. Nicolai Lang
Institute for Theoretical Physics III, University of Stuttgart

June 30th, 2021
SS 2021

Problem 1: Edge modes from Dirac Hamiltonians

Learning objective

In the lecture we argued that both the Chern insulator and the $\mathbb{Z}_2$ topological insulator feature gapless edge modes on boundaries of the system. The phenomenon that a topologically non-trivial bulk entails gapless modes on the surface is known as *bulk-boundary correspondence*. Here you will show that the emergence of these gapless, edge-localized modes already follows from the low-energy description in terms of Dirac Hamiltonians.

Consider an infinite 2D system that is effectively described by a Dirac Hamiltonian with a y-dependent mass term that varies continuously and is negative (positive) in the left (right) half-plane. It therefore must vanish on the x-axis which becomes the boundary that separates the two gapped systems A and B. →

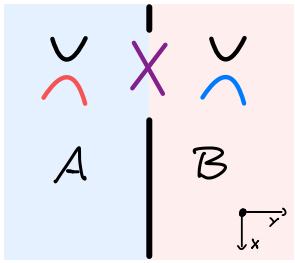

In real space, the Dirac Hamiltonian of this system reads

$$H_{\mathrm{D}} = -i\nabla \cdot \vec{\sigma} + m(y)\,\sigma^z = \begin{pmatrix} m(y) & -i\partial_x - \partial_y \\ -i\partial_x + \partial_y & -m(y) \end{pmatrix} \tag{1}$$

with $\vec{\sigma} = (\sigma^x, \sigma^y)^T$; the functional dependence of $m(y)$ is given in the sketch on the right.

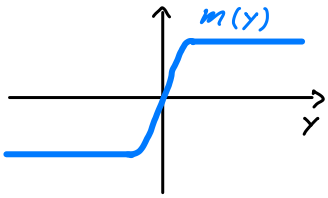

Consequently, the Chern number of the two materials A and B must differ by ± 1 because of the sign change of the Dirac mass at the boundary; remember that

$$C = -\frac{\mathrm{sign}[m(y)]}{2} \tag{2}$$

for a Dirac Hamiltonian. You can think of material B as a trivial insulator with $C = 0$ and of material A as a Chern insulator with $C = 1$; both insulators share an interface at $y = 0$.

a) Use the Hadamard transform $H_{\mathrm{D}} \mapsto U H_{\mathrm{D}} U^\dagger$ with

$$U = \frac{1}{\sqrt{2}} \begin{pmatrix} 1 & 1 \\ 1 & -1 \end{pmatrix} \tag{3}$$

to solve the time-independent Schrödinger equation

$$H_{\mathrm{D}}\Psi(x,y) = E\Psi(x,y) \tag{4}$$

with the two-component spinor $\Psi(x,y)$.

(*Hint:* Make a product ansatz to separate the PDEs after the transformation with U and set the separation constants to zero. Use the behaviour of $m(y)$ sketched above to select a unique, non-diverging solution.)

b) What is the spectrum $E(k_x)$ of the solution and what is its group velocity along the boundary? Where is the solution localized in y-direction?

Problem 2: The sewing matrix expression for the Pfaffian invariant

Learning objective

In the lecture we introduced the Pfaffian invariant as the parity of the vorticity of the Pfaffian in an effective Brillouin zone. This topological $\mathbb{Z}_2$ index characterizes the topological phase of the Kane-Mele model. Here you derive an equivalent expression for the Pfaffian invariant in terms of the *sewing matrix*. This expression is pivotal for the construction of topological insulators in three dimensions.

Let $\{|e_i(\boldsymbol{k})\rangle\}_{i=1\ldots 2n}$ be a globally continuous basis of the valence bundle, i.e., the subspace of filled Bloch states $\mathcal{H}_{\boldsymbol{k}}^{\text{filled}}$ over the Brillouin zone T^2. In the lecture, we defined the Pfaffian index as

$$I = \frac{1}{2\pi i} \oint_{\partial\text{EBZ}} \nabla \log P(\boldsymbol{k}) \cdot \mathrm{d}\boldsymbol{k} \mod 2 = \frac{1}{2\pi i} \oint_{\partial\text{EBZ}} \mathrm{d} \log P(\boldsymbol{k}) \mod 2 \tag{5}$$

with ∂EBZ the boundary of a suitably chosen effective Brillouin zone that does not intersect with the vortices of $P(\boldsymbol{k})$. The latter is given as Pfaffian

$$P(\boldsymbol{k}) = \text{Pf}\,[M(\boldsymbol{k})] \tag{6}$$

of the skew-symmetric matrix

$$M_{ij}(\boldsymbol{k}) = \langle e_i(\boldsymbol{k})|\, \tilde{T}_U\, |e_j(\boldsymbol{k})\rangle \ . \tag{7}$$

$\tilde{T}_U$ denotes the time-reversal operator with $\tilde{T}_U^2 = -\mathbb{1}$ and in the following, $\mathcal{I}$ is the set of TRIMs.

a) Let the *sewing matrix* be defined as

$$w_{ij}(\boldsymbol{k}) = \langle e_i(-\boldsymbol{k})|\, \tilde{T}_U\, |e_j(\boldsymbol{k})\rangle \tag{8}$$

and prove the following properties:

i. $w(\boldsymbol{k})w^\dagger(\boldsymbol{k}) = \mathbb{1}$ ($\rightarrow$ unitarity everywhere on T^2)

ii. $w^T(\boldsymbol{k}) = -w(-\boldsymbol{k})$ ($\rightarrow$ skew-symmetry at TRIMs)

iii. $w(\boldsymbol{K}) = M(\boldsymbol{K})$ for $\boldsymbol{K} \in \mathcal{I}$

iv. $M(-\boldsymbol{k}) = w(\boldsymbol{k}) \cdot M^*(\boldsymbol{k}) \cdot w^T(\boldsymbol{k})$

v. $\det w(\boldsymbol{k}) = P(\boldsymbol{k})/[P(-\boldsymbol{k})]^*$

b) Show that $\det[w(\boldsymbol{k})] = \det[w(-\boldsymbol{k})]$ and use this to prove that

$$\frac{1}{2\pi i} \oint_{\mathcal{C}} \mathrm{d} \log[\det w(\boldsymbol{k})] = 0 \tag{9}$$

for every closed path $\mathcal{C}$ on the Brillouin zone T^2; i.e., $\det w(\boldsymbol{k})$ does not have any vorticity.

(*Hint:* Note that the *non-contractible* loops around the torus T^2 allow for phase windings even in the absence of vortices. To show that even for such loops the above integral vanishes, use that every loop can be continuously deformend into a time-reversal invariant loop, i.e., a loop that is mapped onto itself under $\boldsymbol{k} \mapsto -\boldsymbol{k}$.)

c) For a closed path $\mathcal{C}$ that does not cross zeros of $P(\boldsymbol{k})$, define $L[\mathcal{C}] := \oint_{\mathcal{C}} \mathrm{d} \log P(\boldsymbol{k})$ so that $I = L[\partial \mathrm{EBZ}]/(2\pi i) \mod 2$. Show that

$$(-1)^I = \exp\left\{\frac{L[\mathcal{C}_{1,2}] - L[\mathcal{C}_{3,4}]}{2}\right\} \tag{10}$$

where $\mathcal{C}_{i,j}$ are the two disjoint boundary components of the EBZ (each of which passes through two TRIMs i and j). Each of these paths can be split into two connected components $\mathcal{C}^{\pm}_{i,j}$ that are mapped onto each other under time-reversal:

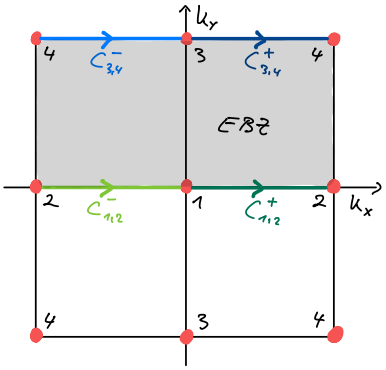

Show that we can decompose the terms in (10) as

$$L[\mathcal{C}_{i,j}] = 2L[\mathcal{C}^+_{i,j}] + \left(L[\mathcal{C}^-_{i,j}] - L[\mathcal{C}^+_{i,j}]\right) . \tag{11}$$

d) To evaluate Eq. (11), show first that

$$\exp L[\mathcal{C}^+_{i,j}] = \frac{\mathrm{Pf}\,[w(\boldsymbol{K}_j)]}{\mathrm{Pf}\,[w(\boldsymbol{K}_i)]} , \tag{12}$$

e) and then

$$L[\mathcal{C}^+_{i,j}] - L[\mathcal{C}^-_{i,j}] = \int_{\mathcal{C}^+_{i,j}} \mathrm{d}\left[\log P(\boldsymbol{k}) - \log P^*(-\boldsymbol{k})\right] . \tag{13}$$

(*Hint:* Use that $|P(\boldsymbol{K})| = 1$ at TRIMs $\boldsymbol{K} \in \mathcal{I}$ and $|P(\boldsymbol{k})| = |P(-\boldsymbol{k})|$ from subtask a).)

f) Use the previous result to derive

$$\exp\left\{\frac{L[\mathcal{C}^+_{i,j}] - L[\mathcal{C}^-_{i,j}]}{2}\right\} = \frac{\sqrt{\det w(\boldsymbol{K}_j)}}{\sqrt{\det w(\boldsymbol{K}_i)}} . \tag{14}$$

(*Hint:* Results from Subtask a) might be helpful.)

g) Combine your results to prove the final expression

$$(-1)^I = \prod_{\boldsymbol{K}\in\mathcal{I}} \frac{\mathrm{Pf}\,[w(\boldsymbol{K})]}{\sqrt{\det w(\boldsymbol{K})}} . \tag{15}$$

This expression allows for the computation of the Pfaffian invariant I based only on the values of the sewing matrix at the TRIMs. Eq. (15) is important because it can be used to generalize the $\mathbb{Z}_2$ invariant to three dimensions and leads naturally to the concept of *weak topological insulators*[1].

(*Hint:* For the validity of Eq. (15) you need the continuity of $\sqrt{\det w(\boldsymbol{k})}$ on T^2 (why?). Give a reason why such a choice for the square root is possible. Furthermore, the identity $(\mathrm{Pf}[A])^2 = \det[A]$ may be useful.)

Problem 3: Edge modes of the Kane-Mele model (Numerics)

Learning objective

A characteristic feature of phases with topologically non-trivial bands is the emergence of gapless edge modes on boundaries of the system (see also Problem 1). These modes make the system conducting on the boundaries whereas the bulk is a gapped insulator. Because it is well-known that one doesn't really understand what one cannot program, here you study the edge modes of the Kane-Mele topological insulator numerically.

The many-body Hamiltonian of the Kane-Mele model (without Rashba coupling) reads

$$\hat{H}_{\mathrm{KM}} = \sum_{\langle i,j\rangle,\alpha} c^\dagger_{i\alpha} c_{j\alpha} + m \sum_{i,\alpha} \epsilon_i c^\dagger_{i\alpha} c_{i\alpha} + \lambda_{\mathrm{SO}} \sum_{\langle\langle i,j\rangle\rangle,\alpha,\beta} i\eta_{ji}\, c^\dagger_{i\alpha} \mu^z_{\alpha\beta} c_{j\beta} \tag{16}$$

where i, j run over sites on the honeycomb lattice, $\alpha \in \{\uparrow, \downarrow\}$ is the spin in the z-basis and $\langle i, j\rangle$ and $\langle\langle i, j\rangle\rangle$ denote nearest neighbour and next-nearest neighbour pairs, respectively. ϵ_i is ± 1 on the two sublattices of the honeycomb lattice and $\eta_{ji} = \pm 1$ is chosen positive for an electron that makes a right-turn when hopping from j to i. μ^i ($i = x, y, z$) are Pauli matrices that act on the spin degree of freedom.

Here we consider the Hamiltonian on a finite strip with $L_{x/y}$ unit cells in x/y-direction, periodic boundary conditions in y- and *open* boundary conditions in x-direction:

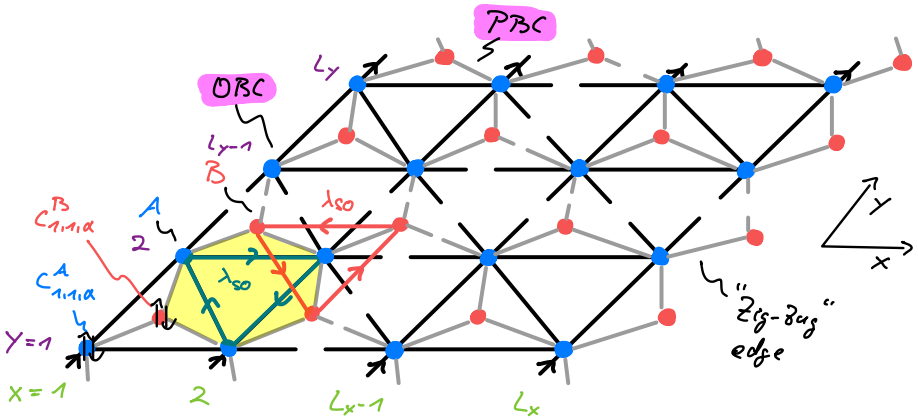

Note that this choice of boundary conditions leads to "zig-zag" type edges.

[1] L. Fu, C. L. Kane, and E. J. Mele, *Topological Insulators in Three Dimensions*, PRL **98**, 106803 (2007), https://doi.org/10.1103/PhysRevLett.98.106803

a) Since the strip is only periodic in y-direction, we consider the system as a 1D chain in y-direction with very large ($2 \times 2 \times L_x$) unit cell.

Fourier transform Eq. (16) in y-direction and show that it takes the form

$$\hat{H}_{\text{KM}} = \sum_{k_y \in \text{BZ}} \mathbf{\Psi}^\dagger_{k_y} H(k_y) \mathbf{\Psi}_{k_y} \tag{17}$$

with $4L_x$-component spinor

$$\mathbf{\Psi}_{k_y} = \begin{pmatrix} \tilde{c}^A_{1,k_y,\uparrow} & \tilde{c}^B_{1,k_y,\uparrow} & \dots & \tilde{c}^A_{L_x,k_y,\uparrow} & \tilde{c}^B_{L_x,k_y,\uparrow} & \tilde{c}^A_{1,k_y,\downarrow} & \tilde{c}^B_{1,k_y,\downarrow} & \dots & \tilde{c}^A_{L_x,k_y,\downarrow} & \tilde{c}^B_{L_x,k_y,\downarrow} \end{pmatrix}^T .$$

Here, $\tilde{c}^\beta_{x,k_y,\alpha}$ denotes the fermion mode at x-position $x = 1 \dots L_x$ with y-momentum k_y and spin $\alpha \in \{\uparrow, \downarrow\}$ on sublattice site $\beta \in \{A, B\}$.

(*Hint:* The generic site index i in the modes $c_{i\alpha}$ in Eq. (16) must be carefully translated into a triple $i = (x, y, \beta)$ with $x = 1 \dots L_x$ and $y = 1 \dots L_y$ and $\beta \in \{A, B\}$ taking into account the connectivity of the honeycomb lattice (i.e., $c_{i\alpha} = c^\beta_{x,y,\alpha}$), see the sketch above; then a discrete Fourier transform in y yields the modes $\tilde{c}^\beta_{x,k_y,\alpha}$.)

The Bloch Hamiltonian in Eq. (17) is a $4L_x \times 4L_x$-matrix

$$H(k_y) = \begin{pmatrix} H_\uparrow(k_y) & 0 \\ 0 & H_\downarrow(k_y) \end{pmatrix} \tag{18}$$

$$\text{with} \quad H_\alpha(k_y) = \begin{pmatrix} G_\alpha(k_y) & D^\dagger_\alpha(k_y) & 0 & 0 & \dots \\ D_\alpha(k_y) & G_\alpha(k_y) & D^\dagger_\alpha(k_y) & 0 & \ddots \\ 0 & D_\alpha(k_y) & G_\alpha(k_y) & D^\dagger_\alpha(k_y) & \ddots \\ \vdots & \ddots & \ddots & \ddots & \ddots \end{pmatrix} \tag{19}$$

and depends on the y-momentum $0 \le k_y < 2\pi$. It can be interpreted as single particle Hamiltonian of a 1D chain of length L_x with two sublattice sites and spinful fermions.

The blocks take the form

$$G_\alpha(k_y) = \begin{pmatrix} m - 2\lambda^\alpha_{\text{SO}} \sin(k_y) & 1 + e^{-ik_y} \\ 1 + e^{ik_y} & -m + 2\lambda^\alpha_{\text{SO}} \sin(k_y) \end{pmatrix} \tag{20}$$

$$\text{and} \quad D_\alpha(k_y) = \begin{pmatrix} i\lambda^\alpha_{\text{SO}}(1 - e^{ik_y}) & 1 \\ 0 & -i\lambda^\alpha_{\text{SO}}(1 - e^{ik_y}) \end{pmatrix} \tag{21}$$

where we define $\lambda^\uparrow_{\text{SO}} = +\lambda_{\text{SO}}$ and $\lambda^\downarrow_{\text{SO}} = -\lambda_{\text{SO}}$.

Use your favourite programming language (`C++`, `Python`, `Julia`, `Mathematica`, `Matlab`, ...) to construct and diagonalize the matrix $H(k_y)$ as a function of k_y for given parameters L_x, m and λ_{SO} (henceforth we assume $L_y \to \infty$ and choose $k_y \in [0, 2\pi)$ continuously). You should have access to both eigenvalues and the corresponding eigenvectors.

(*Hint:* It is useful to diagonalize the two spin sectors $H_\alpha(k_y)$ separately and plot their spectra with different colors in the same plots to distinguish and compare the spin-polarized bands.)

b) Let us start with graphene. Set $L_x = 50$ and $m = 0 = \lambda_{\text{SO}}$ and plot the full spectrum of $H(k_y)$ over the Brillouin zone $k_y \in [0, 2\pi)$. You should see (projections of) the two Dirac cones that make graphene a semimental. Note that the tips of the cones are connected by two flat bands; this is a peculiar feature of zig-zag edges as already mentioned in the first paper by Kane & Mele[2].

c) Now add a small ($m \approx 0.2$) staggered potential m. Both Dirac cones should obtain a gap. However, there are no gapless ege modes since the spin-polarized bands have no Chern number (as we already know from the Haldane model).

d) Switch off the staggered potential and open a gap using the Kane-Mele spin-orbit coupling instead ($\lambda_{\text{SO}} \approx 0.03$). In contrast to the previous subtask, the spectrum now features four crossing gapless bands (do you see four?); these are *helical edge states* (as you will verify below) and make the strip conducting on the edges. Compare your result to Kane & Mele's plot (Figure 1) in [2].

e) Now start to add in addition the staggered potential and observe how the two spin-manifolds separate (use $\lambda_{\text{SO}} = 0.06$ to compare with the original paper). In the topological phase you should see four separate gapless bands crossing at four distinct points. Plot the spectrum in the topological phase ($m = 0.1$), at the critical point ($m = 3\sqrt{3}\,\lambda_{\text{SO}}$), and in the trivial phase ($m = 0.4$) by ramping up m. Compare your spectra to Kane & Mele's result (Figure 1) in their follow-up paper[3]; in particular, focus on the region where the gapless bands connect to the bulk. Can you explain the differences?

f) We focus now on the four crossings of the edge bands. Consider a system in the topological phase close to the phase transition ($m = 0.25$, $\lambda_{\text{SO}} = 0.06$) and compare the spectrum for a wide ($L_x = 50$) and a narrow strip ($L_x = 10$). Which edge modes gap out for small systems, which do not? Can you explain why?

g) Finally we should identify the states of the gapless bands as *edge states*. To do so, select four *eigenvectors* of $H(k_y)$ in the topological phase (two for each $H_{\uparrow/\downarrow}(k_y)$) on the four bands that cross zero energy (= Fermi energy) with eigenenergies close to zero (this determines k_y).

The eigenstates of $H_{\uparrow/\downarrow}(k_y)$ have $2L_x$ components enumerating the sublattice sites in x-direction (i.e., across the strip). Plot the modulus of their amplitudes as a function of the x-position. Use this to correlate (1) where the states on the four crossing bands are located in x-direction, (2) their spin polarization, and (3) their group velocity in y-direction.

It is their exponential localization on the edges of the strip combined with their gapless nature that marks them as *gapless edge modes/states*. Physically, the strip has conducting channels (where group velocity and spin-polarization are locked) on its boundary while being a gapped insulator in the bulk.

To demonstrate that the edge states are special you can plot a few states picked from the gapped bulk spectrum for comparison (e.g., the states with highest energy in the spectrum for some k_y).

[2] C. L. Kane and E. J. Mele, *Quantum Spin Hall Effect in Graphene*, PRL **95**, 226801 (2005), https://doi.org/10.1103/PhysRevLett.95.226801

[3] C. L. Kane and E. J. Mele, *Z_2 Topological Order and the Quantum Spin Hall Effect*, PRL **95**, 146802 (2005), https://doi.org/10.1103/PhysRevLett.95.146802